

Crystal structure, Hirshfeld surface analysis and interaction energy calculation of 1-decyl-2,3-dihydro-1*H*-benzimidazol-2-one

Younesse Ait Elmachkouri,^{a,b} Asmaa Saber,^b Ezaddine Irrou,^{a,b} Bushra Amer,^{c*} Joel T. Mague,^d Tuncer Hökelek,^e Mohamed Labd Taha,^a Nada Kheira Sebbar^{a,b} and El Mokhtar Essassi^b

Received 6 April 2021

Accepted 21 April 2021

Edited by M. Weil, Vienna University of Technology, Austria

Keywords: crystal structure; C—H... π (ring) interaction; dihydroimidazole; Hirshfeld surface analysis.

CCDC reference: 2079158

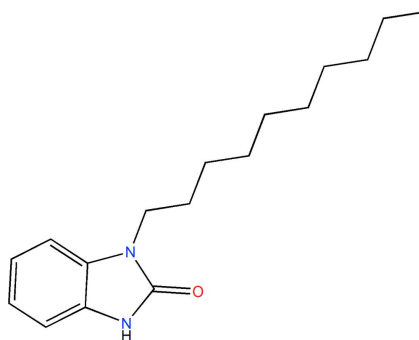
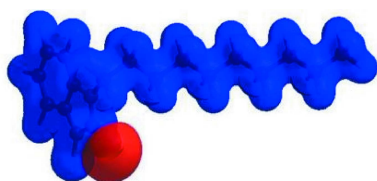
Supporting information: this article has supporting information at journals.iucr.org/e

^aLaboratoire de Chimie Appliquée et Environnement, Equipe de Chimie Bioorganique Appliquée, Faculté des Sciences, Université Ibn Zohr, Agadir, Morocco, ^bLaboratoire de Chimie Organique Hétérocyclique URAC 21, Pôle de Compétence Pharmacochimie, Av. Ibn Battouta, BP 1014, Faculté des Sciences, Université Mohammed V, Rabat, Morocco, ^cFaculty of Medicine and Health Sciences, Sana'a University, San'a, Yemen, ^dDepartment of Chemistry, Tulane University, New Orleans, LA 70118, USA, and ^eDepartment of Physics, Hacettepe University, 06800 Beytepe, Ankara, Turkey.
*Correspondence e-mail: Bushraamer2014@gmail.com

The title molecule, C₁₇H₂₆N₂O, adopts an L-shaped conformation, with the straight *n*-decyl chain positioned nearly perpendicular to the dihydrobenzimidazole moiety. The dihydrobenzimidazole portion is not quite planar as there is a dihedral angle of 1.20 (6)° between the constituent planes. In the crystal, N—H...O hydrogen bonds form inversion dimers, which are connected into the three-dimensional structure by C—H...O hydrogen bonds and C—H... π (ring) interactions. Hirshfeld surface analysis indicates that the most important contributions for the crystal packing are from H...H (75.9%), H...C/C...H (12.5%) and H...O/O...H (7.0%) interactions. Based on computational chemistry using the CE-B3LYP/6-31 G(d,p) energy model, C—H...O hydrogen bond energies are -74.9 (for N—H...O) and -42.7 (for C—H...O) kJ mol⁻¹.

1. Chemical context

Benzimidazol-2-one derivatives constitute an important class of heterocyclic systems. They are used as precursors for the preparation of novel *N*-substituted benzimidazol-2-one derivatives with potential biological and pharmacological properties (Lakhrissi *et al.*, 2008; Saber *et al.*, 2019; Mamedov *et al.*, 2017), including antitumor (Khodarahmi *et al.*, 2005), antibacterial (Saber *et al.*, 2020a; Vira *et al.*, 2010), anti-HIV (Barreca *et al.*, 2007), and antitrichinellosis (Mavrova *et al.*, 2005) activities.



In continuation of our investigations on the synthesis, physico-chemical characterization and biological properties of novel *N*-substituted benzimidazol-2-one derivatives, we have

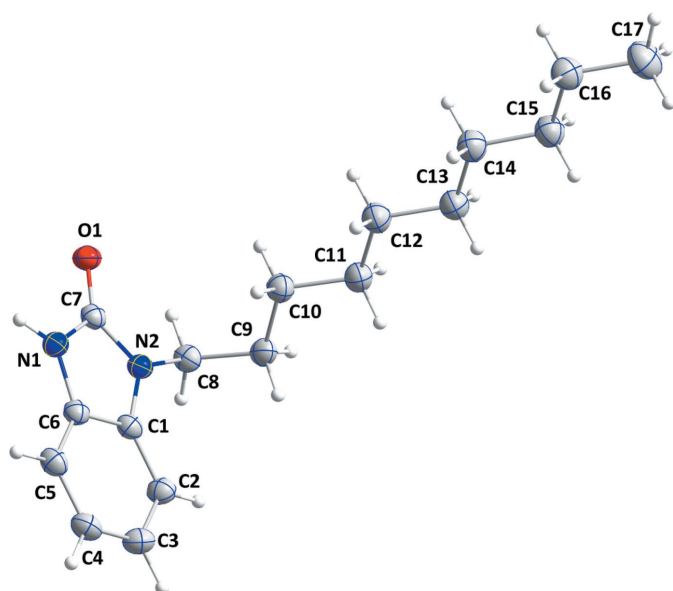


Figure 1
The asymmetric unit of the title compound with the atom-numbering scheme. Displacement ellipsoids are drawn at the 50% probability level.

studied the reaction of 1-bromodecane with 1-isopropenyl-1*H*-1,3-benzimidazol-2(3*H*)-one under phase-transfer catalysis conditions (Saber *et al.*, 2020*b*; Srhir *et al.*, 2020), We report herein the synthesis, and the molecular and crystal structures along with the Hirshfeld surface analysis and the intermolecular interaction energies of the title compound, C₁₇H₂₆N₂O, (I).

2. Structural commentary

The title molecule adopts an L-shaped conformation with the straight *n*-decyl chain arranged nearly perpendicular to the dihydrobenzimidazole portion, as indicated by the C1–N2–

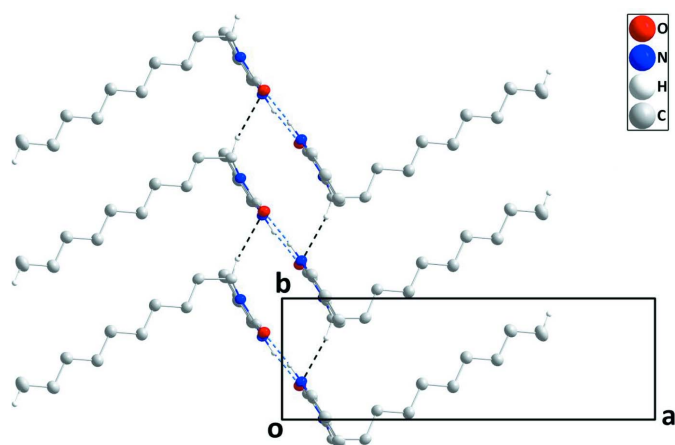


Figure 2
A portion of one chain viewed along the *c*-axis direction with N–H···O and C–H···O hydrogen bonds depicted, respectively, by blue and black dashed lines. H atoms not involved in hydrogen bonding were omitted for clarity.

Table 1
Hydrogen-bond geometry (Å, °).

Cg2 is the centroid of the C1–C6 ring.

<i>D</i> –H··· <i>A</i>	<i>D</i> –H	H··· <i>A</i>	<i>D</i> ··· <i>A</i>	<i>D</i> –H··· <i>A</i>
N1–H1···O1 ⁱⁱ	0.923 (16)	1.932 (16)	2.8393 (12)	167.0 (13)
C8–H8A···O1 ^{viii}	0.995 (13)	2.573 (13)	3.4648 (12)	149.1 (9)
C17–H17C···Cg2 ^v	1.00 (2)	2.985 (19)	3.6656 (17)	126.0 (14)

Symmetry codes: (ii) $-x, -y + 1, -z + 1$; (v) $-x + 1, -y + 1, -z + 1$; (viii) $x, y - 1, z$.

C8–C9 torsion angle of $-75.91 (12)^\circ$ (Fig. 1). The dihydrobenzimidazole portion is not planar, as indicated by the dihedral angle of $1.20 (6)^\circ$ between the constituent planes.

3. Supramolecular features

In the crystal of (I), inversion dimers are formed by N1–H1···O1 hydrogen bonds (Table 1) that are linked into chains extending parallel to the *b* axis by C8–H8A···O1 hydrogen bonds (Table 1, Fig. 2). The alkyl groups extend from both sides of the chain and intercalate with alkyl groups of adjacent chains while linking them together through C17–H17C···Cg2 interactions (Table 2, Fig. 3).

4. Hirshfeld surface analysis

In order to visualize the intermolecular interactions in the crystal of the title compound, a Hirshfeld surface (HS) analysis (Hirshfeld, 1977) was carried out using *Crystal Explorer 17.5* (Turner *et al.*, 2017). A view of the three-dimensional Hirshfeld surface of (I), plotted over d_{norm} and the electrostatic potential map are shown in Fig. 4*a* and *b*, respectively. The shape-index of the HS reveals that there are no π – π interactions in (I), as shown in Fig. 4*c*. The overall two-

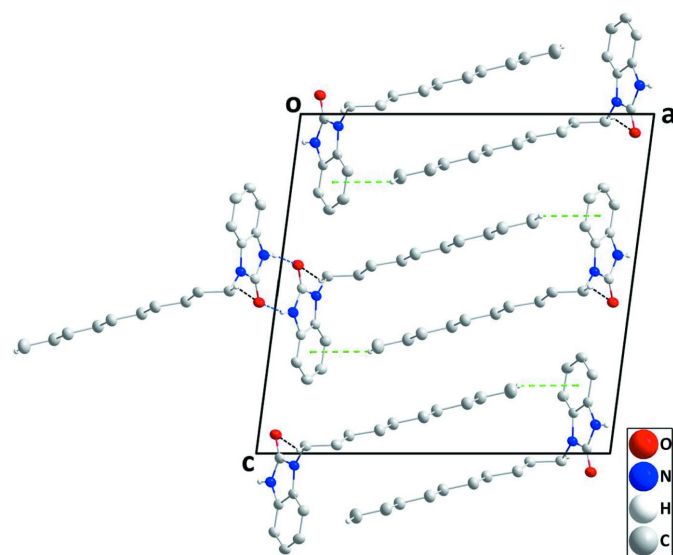


Figure 3
Packing viewed along the *b*-axis direction with hydrogen bonds depicted as in Fig. 2 and C–H··· π (ring) interactions by green dashed lines. H atoms not involved in hydrogen bonding were omitted for clarity.

dimensional fingerprint plot, Fig. 5a, and those delineated into H···H, H···C/C···H, H···O/O···H, H···N/N···H, C···O/O···C, N···O/O···N, C···N/N···C and C···C contacts (McKinnon *et al.*, 2007) are illustrated in Fig. 5b–i, respectively, together with their relative contributions to the Hirshfeld surface. The most important interaction is H···H (Table 2) contributing 75.9% to the overall crystal packing, which is reflected in Fig. 5b as widely scattered points of high density due to the large hydrogen content of the molecule, with the tip at $d_e = d_i = 1.08$ Å. In the presence of C–H··· π interactions, the pair of characteristic wings are seen in the fingerprint plot (Fig. 5c) delineated into H···C/C···H contacts (12.5% contribution; Table 2), with the tips at $d_e + d_i = 2.66$ Å. The

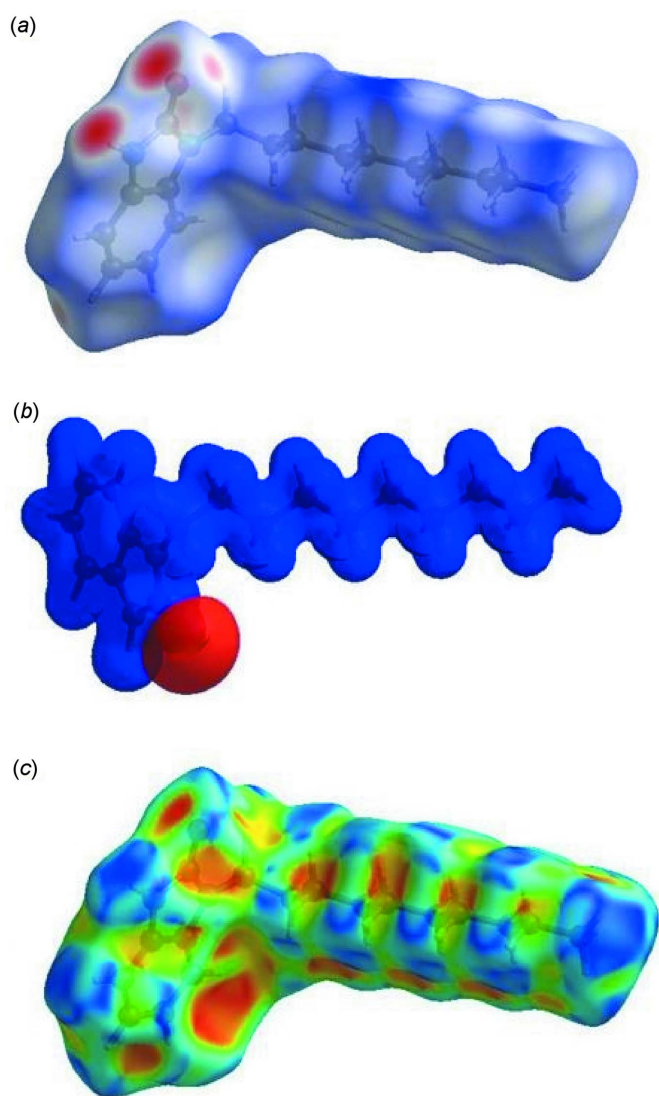


Figure 4
(a) View of the three-dimensional Hirshfeld surface of the title compound, plotted over d_{norm} in the range of -0.5871 to 1.6590 a.u. (b) View of the three-dimensional Hirshfeld surface of the title compound plotted over electrostatic potential energy in the range -0.0500 to 0.0500 a.u. using the STO-3 G basis set at the Hartree–Fock level of theory. (c) Hirshfeld surface of the title compound plotted over shape-index.

Table 2
Selected interatomic distances (Å).

O1···C1 ⁱ	3.2784 (12)	H9B···H11B	2.53 (2)
O1···N1 ⁱⁱ	2.8394 (11)	H10A···H12A	2.55 (2)
C4···O1 ⁱⁱⁱ	3.2820 (14)	H10B···H12B	2.58 (2)
O1···H8B	2.486 (11)	H11A···H13A	2.58 (2)
O1···H1 ⁱⁱ	1.934 (16)	H11A···H16A ^v	2.43 (2)
O1···H8A ^{iv}	2.571 (11)	H11B···H13B	2.51 (2)
H4···O1 ⁱⁱⁱ	2.417 (13)	H12A···H14A	2.55 (2)
N1···H8A ^{iv}	2.878 (12)	H12A···H15A ^v	2.57 (2)
N1···H8B ⁱ	2.949 (12)	H12B···H14B	2.53 (2)
N2···H10A	2.843 (14)	H13A···H15A	2.55 (2)
C7···C7 ⁱ	3.2937 (14)	H13A···H14A ^v	2.52 (2)
C2···H17C ^v	2.90 (2)	H13B···H15B	2.57 (2)
C7···H1 ⁱⁱ	2.828 (16)	H13B···H16B ^{vii}	2.47 (2)
C7···H8A ^{iv}	2.774 (11)	H14A···H16A	2.51 (2)
H2···H9A	2.572 (19)	H14B···H16B	2.56 (2)
H2···H17A ^{vi}	2.34 (2)	H14B···H16B ^{vii}	2.54 (2)
H8B···H10B	2.507 (18)	H15A···H17A	2.60 (2)
H9A···H11A	2.550 (19)	H15B···H17B	2.54 (2)

Symmetry codes: (i) $-x, -y, -z + 1$; (ii) $-x, -y + 1, -z + 1$; (iii) $x, -y + \frac{1}{2}, z + \frac{1}{2}$; (iv) $x, y + 1, z$; (v) $-x + 1, -y + 1, -z + 1$; (vi) $-x + 1, -y, -z + 1$; (vii) $-x + 1, y - \frac{1}{2}, -z + \frac{1}{2}$.

pair of the scattered points of spikes in the fingerprint plot delineated into H···O/O···H contacts, Fig. 5d, with a 7.0% contribution to the HS, has a distribution of points with the tips at $d_e + d_i = 1.83$ Å. The H···N/N···H contacts, Fig. 5e, with a 2.3% contribution to the HS have the tips at $d_e + d_i = 2.92$ Å. The C···O/O···C contacts, Fig. 5f, with a 1.2% contribution to the HS appear as a pair of scattered points of

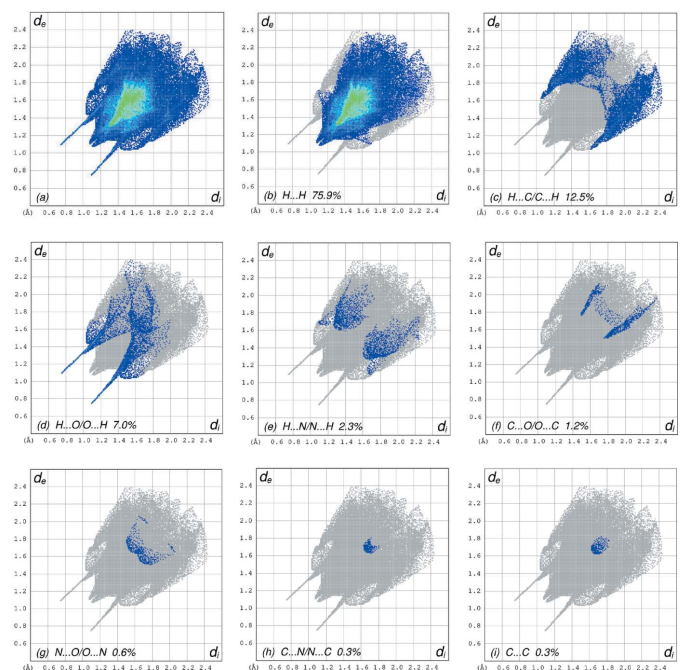


Figure 5
The full two-dimensional fingerprint plots for the title compound, showing (a) all interactions, and delineated into (b) H···H, (c) H···C/C···H, (d) H···O/O···H, (e) H···N/N···H, (f) C···O/O···C, (g) N···O/O···N, (h) C···N/N···C and (i) C···C interactions. The d_i and d_e values are the closest internal and external distances (in Å) from given points on the Hirshfeld surface contacts.

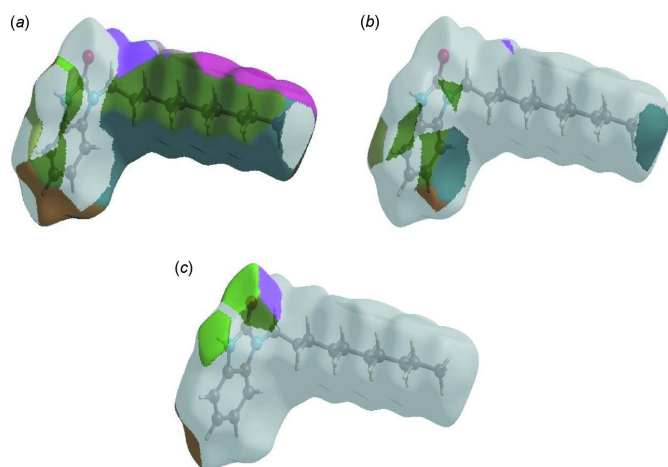


Figure 6
The Hirshfeld surface representations with the function d_{norm} plotted onto the surface for (a) $\text{H}\cdots\text{H}$, (b) $\text{H}\cdots\text{C}/\text{C}\cdots\text{H}$ and (c) $\text{H}\cdots\text{O}/\text{O}\cdots\text{H}$ interactions.

spikes with the tips at $d_e + d_i = 3.25 \text{ \AA}$. Finally, the $\text{N}\cdots\text{O}/\text{O}\cdots\text{N}$ (Fig. 5g), $\text{N}\cdots\text{C}/\text{C}\cdots\text{N}$ (Fig. 5h) and $\text{C}\cdots\text{C}$ (Fig. 5i) contacts have 0.6%, 0.3% and 0.3% contributions, respectively, to the HS with low-density distributions of points.

The Hirshfeld surface representations with the function d_{norm} plotted onto the surface are shown for the $\text{H}\cdots\text{H}$, $\text{H}\cdots\text{C}/\text{C}\cdots\text{H}$ and $\text{H}\cdots\text{O}/\text{O}\cdots\text{H}$ interactions in Fig. 6a–c, respectively.

The Hirshfeld surface analysis confirms the importance of H-atom contacts in establishing the packing. The large number of $\text{H}\cdots\text{H}$, $\text{H}\cdots\text{C}/\text{C}\cdots\text{H}$ and $\text{H}\cdots\text{O}/\text{O}\cdots\text{H}$ interactions suggest that van der Waals interactions play the major role in the crystal packing (Hathwar *et al.*, 2015).

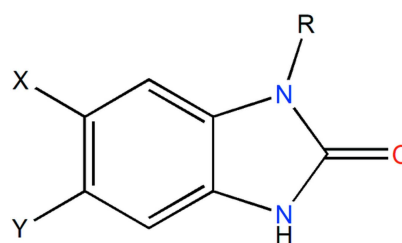
5. Interaction energy calculations

The intermolecular interaction energies were calculated using the CE-B3LYP/6-31G(d,p) energy model available in *Crystal Explorer 17.5* (Turner *et al.*, 2017), where a cluster of molecules is used by applying crystallographic symmetry operations with respect to a selected central molecule within a default radius of 3.8 \AA (Turner *et al.*, 2014). The total intermolecular energy (E_{tot}) is the sum of electrostatic (E_{ele}), polarization (E_{pol}), dispersion (E_{dis}) and exchange-repulsion (E_{rep}) energies (Turner *et al.*, 2015) with scale factors of 1.057, 0.740, 0.871 and 0.618, respectively (Mackenzie *et al.*, 2017). Hydrogen-bonding interaction energies (in kJ mol^{-1}) were calculated as -91.9 (E_{ele}), -21.4 (E_{pol}), -14.5 (E_{dis}), 82.1 (E_{rep}) and -74.9 (E_{tot}) for $\text{N1}-\text{H1}\cdots\text{O1}$ and -9.2 (E_{ele}), -0.6 (E_{pol}), -65.8 (E_{dis}), 39.9 (E_{rep}) and -42.7 (E_{tot}) for $\text{C8}-\text{H8A}\cdots\text{O1}$.

6. Database survey

A search of the Cambridge Structural Database (CSD2021, updated to 2 February, 2021; Groom *et al.*, 2016) using the fragment below, where $X = Y = \text{H}$, $R = (\text{CH}_2)_4\text{C}$, found nine

similar structures. These are IJUGIE [$X = Y = \text{H}$, $R = (\text{CH}_2)_8\text{CH}_3$; Ouzidan *et al.*, 2011a], SECBUZ [$X = Y = \text{H}$, $R = (\text{CH}_2)_{11}\text{CH}_3$; Belaziz *et al.*, 2012b], ZANXET [$X = Y = \text{H}$, $R = (\text{CH}_2)_7\text{CH}_3$; Belaziz *et al.*, 2012a], OCAJIN [$X = \text{H}$, $Y = \text{Cl}$, $R = (\text{CH}_2)_8\text{CH}_3$; Kandri Rodi *et al.*, 2011], ULEDEV [$X = \text{H}$, $Y = \text{NO}_2$, $R = (\text{CH}_2)_7\text{CH}_3$; Ouzidan *et al.*, 2011b], ULEPIL [$X = \text{H}$, $Y = \text{NO}_2$, $R = (\text{CH}_2)_9\text{CH}_3$; Ouzidan *et al.*, 2011c], ULEZAN [$X = \text{H}$, $Y = \text{NO}_2$, $R = (\text{CH}_2)_8\text{CH}_3$; Ouzidan *et al.*, 2011d], QUDJAC [$X = \text{NO}_2$, $Y = \text{H}$, $R = (\text{CH}_2)_8\text{CH}_3$; Venkatraman & Fronczek, 2015] and YAGQII [$X = \text{NO}_2$, $Y = \text{H}$, $R = (\text{CH}_2)_9\text{CH}_3$; Ouzidan *et al.*, 2011e]. In all of these molecules, the long alkyl substituent has a straight shape rather than being folded back on itself. This is likely driven by packing considerations as straight alkyl chains can efficiently intercalate, thereby minimizing void space in the crystal.



7. Synthesis and crystallization

The title compound was prepared in two steps. In the first step, 1-bromodecane (11.4 mmol) was added to a mixture of 1-isopropenyl-1*H*-1,3-benzimidazol-2(3*H*)-one (5.7 mmol), potassium hydroxide (5.7 mmol) and tetra-*n*-butyl ammonium bromide (0.15 mmol) in CH_2Cl_2 (15 ml). Stirring was continued at room temperature for 48 h. The formed salts were removed by filtration, and the filtrate was concentrated under reduced pressure. The residue obtained was purified by recrystallization from ethanol to obtain 1-(prop-1-en-2-yl)-3-decyl-2,3-dihydro-1*H*-benzimidazol-2(3*H*)-one in 82% yield. In the second step, 1-(prop-1-en-2-yl)-3-decyl-2,3-dihydro-1*H*-benzimidazol-2-one (7.0 mmol) was dissolved in a mixture of dimethylformamide (DMF; 10 ml) and cold sulfuric acid (15 ml, 50% wt). The reaction mixture was stirred at room temperature for 12 h. The precipitate obtained was filtered off and washed with water and subsequently dried. The resulting residue was purified by recrystallization from ethanol to obtain colourless crystals in 75% yield.

^1H NMR (300 MHz, $\text{DMSO}-d_6$): 0.87 (*t*, 3H, CH_3); 1.25–1.67 (*m*, 16H, CH_2); 2.80–3.04 (*m*, 2H, CH_2); 6.99–7.12 (*m*, 4H, H_{arom}); 10.58 (*s*, 1H, NH). ^{13}C NMR (75 MHz, $\text{DMSO}-d_6$): 14.14 (CH_3); 22.70, 26.90, 28.44, 29.31, 29.51, 29.56, 29.74, 31.90, 41.44 (CH_2); 107.84, 108.45, 121.20, 121.65 (CH_{arom}); 128.52, 129.64 (Cq), 153.43 (C=O).

8. Refinement

Crystal, data collection and refinement details are presented in Table 3. Hydrogen atoms were located in difference-Fourier maps and were freely refined.

Table 3
Experimental details.

Crystal data	
Chemical formula	C ₁₇ H ₂₆ N ₂ O
<i>M_r</i>	274.40
Crystal system, space group	Monoclinic, <i>P</i> ₂ / <i>c</i>
Temperature (K)	150
<i>a</i> , <i>b</i> , <i>c</i> (Å)	17.3256 (5), 5.5662 (2), 16.7244 (5)
β (°)	97.433 (1)
<i>V</i> (Å ³)	1599.31 (9)
<i>Z</i>	4
Radiation type	Cu <i>K</i> α
μ (mm ⁻¹)	0.55
Crystal size (mm)	0.26 × 0.17 × 0.10
Data collection	
Diffractometer	Bruker D8 VENTURE PHOTON 100 CMOS
Absorption correction	Numerical (<i>SADABS</i> ; Krause <i>et al.</i> , 2015)
<i>T</i> _{min} , <i>T</i> _{max}	0.88, 0.95
No. of measured, independent and observed [<i>I</i> > 2 σ (<i>I</i>)] reflections	11457, 3082, 2857
<i>R</i> _{int}	0.028
(<i>sin</i> θ / λ) _{max} (Å ⁻¹)	0.618
Refinement	
<i>R</i> [<i>F</i> ² > 2 σ (<i>F</i> ²)], <i>wR</i> (<i>F</i> ²), <i>S</i>	0.041, 0.101, 1.08
No. of reflections	3082
No. of parameters	286
H-atom treatment	All H-atom parameters refined
$\Delta\rho_{\text{max}}$, $\Delta\rho_{\text{min}}$ (e Å ⁻³)	0.19, -0.26

Computer programs: *APEX3* and *SAINT* (Bruker, 2016), *SAINT* (Bruker, 2016), *SHELXT/5* (Sheldrick, 2015a), *SHELXL2018/3* (Sheldrick, 2015b), *DIAMOND* (Brandenburg & Putz, 2012) and *publCIF* (Westrip, 2010).

Acknowledgements

Author contribution are as follows. Conceptualization, AS, MLT, NKS; methodology, BA and YAE; investigation, YAE, IE, JTM and TH; writing (original draft), JTM, TH and NKS; writing (review and editing of the manuscript), YAE and IE; visualization, MLT and EME; resources, EME and AS; supervision, BA and NKS.

Funding information

The support of NSF–MRI grant No. 1228232 for the purchase of the diffractometer and Tulane University for support of the Tulane Crystallography Laboratory are gratefully acknowledged. TH is grateful to Hacettepe University Scientific Research Project Unit (grant No. 013 D04 602 004).

References

Barreca, M. L., Rao, A., De Luca, L., Iraci, N., Monforte, A. M., Maga, G., De Clercq, E., Pannecouque, C., Balzarini, J. & Chimirri, A. (2007). *Bioorg. Med. Chem. Lett.* **17**, 1956–1960.
 Belaziz, D., Kandri Rodi, Y., Essassi, E. M. & El Ammari, L. (2012a). *Acta Cryst.* **E68**, o1276.
 Belaziz, D., Kandri Rodi, Y., Ouazzani Chahdi, F., Essassi, E. M., Saadi, M. & El Ammari, L. (2012b). *Acta Cryst.* **E68**, o3069.
 Brandenburg, K. & Putz, H. (2012). *DIAMOND*, Crystal Impact GbR, Bonn, Germany.

Bruker (2016). *APEX3* and *SAINT*. Bruker AXS Inc., Madison, Wisconsin, USA.
 Groom, C. R., Bruno, I. J., Lightfoot, M. P. & Ward, S. C. (2016). *Acta Cryst.* **B72**, 171–179.
 Hathwar, V. R., Sist, M., Jørgensen, M. R. V., Mamakhel, A. H., Wang, X., Hoffmann, C. M., Sugimoto, K., Overgaard, J. & Iversen, B. B. (2015). *IUCrJ*, **2**, 563–574.
 Hirshfeld, H. L. (1977). *Theor. Chim. Acta*, **44**, 129–138.
 Kandri Rodi, Y., Ouazzani Chahdi, F., Essassi, E. M., Luis, S. V., Bolte, M. & El Ammari, L. (2011). *Acta Cryst.* **E67**, o3340–o3341.
 Khodarahmi, G. A., Chen, C. S., Hakimelahi, G. H., Tseng, C. T. & Chern, J. W. (2005). *J. Iran. Chem. Soc.* **2**, 124–134.
 Krause, L., Herbst-Irmer, R., Sheldrick, G. M. & Stalke, D. (2015). *J. Appl. Cryst.* **48**, 3–10.
 Lakhri, B., Benksim, A., Massoui, M., Essassi, E. M., Lequart, V., Joly, N., Beaupère, D., Wadouachi, A. & Martin, P. (2008). *Carbohydr. Res.* **343**, 421–433.
 Mackenzie, C. F., Spackman, P. R., Jayatilaka, D. & Spackman, M. A. (2017). *IUCrJ*, **4**, 575–587.
 Mamedov, V. A., Zhukova, N. A. & Sinyashin, O. G. (2017). *Mendeleev Commun.* **27**, 1–11.
 Mavrova, A. T., Anichina, K. K., Vuchev, D. I., Tsenov, J. A., Kondeva, M. S. & Micheva, M. K. (2005). *Bioorg. Med. Chem.* **13**, 5550–5559.
 McKinnon, J. J., Jayatilaka, D. & Spackman, M. A. (2007). *Chem. Commun.* pp. 3814–3816.
 Ouzidan, Y., Kandri Rodi, Y., Butcher, R. J., Essassi, E. M. & El Ammari, L. (2011a). *Acta Cryst.* **E67**, o283.
 Ouzidan, Y., Kandri Rodi, Y., Essassi, E. M., El Ammari, L., Fronczek, F. R. & Venkatraman, R. (2011d). *Acta Cryst.* **E67**, o669.
 Ouzidan, Y., Kandri Rodi, Y., Essassi, E. M., Luis, S. V., Bolte, M. & El Ammari, L. (2011e). *Acta Cryst.* **E67**, o2937.
 Ouzidan, Y., Kandri Rodi, Y., Ladeira, S., Essassi, E. M. & Ng, S. W. (2011c). *Acta Cryst.* **E67**, o613.
 Ouzidan, Y., Kandri Rodi, Y., Saffon, N., Essassi, E. M. & Ng, S. W. (2011b). *Acta Cryst.* **E67**, o558.
 Saber, A., Sebbar, N. K. & Essassi, E. M. (2019). *J. Mar. Chem. Heterocycl.* **18**, 1–50.
 Saber, A., Sebbar, N. K., Hökelek, T., Labd Taha, M., Mague, J. T., Hamou Ahabchane, N. & Essassi, E. M. (2020a). *Acta Cryst.* **E76**, 95–101.
 Saber, A., Sebbar, N. K., Sert, Y., Alzaqri, N., Hökelek, T., El Ghayati, L., Talbaoui, A., Mague, J. T., Baba, Y. F., Urrutigoity, M. & Essassi, E. M. (2020b). *J. Mol. Struct.* **1200**, 127174.
 Sheldrick, G. M. (2015a). *Acta Cryst.* **A71**, 3–8.
 Sheldrick, G. M. (2015b). *Acta Cryst.* **C71**, 3–8.
 Srhir, M., Sebbar, N. K., Hökelek, T., Moussaif, A., Mague, J. T., Hamou Ahabchane, N. & Essassi, E. M. (2020). *Acta Cryst.* **E76**, 370–376.
 Turner, M. J., Grabowsky, S., Jayatilaka, D. & Spackman, M. A. (2014). *J. Phys. Chem. Lett.* **5**, 4249–4255.
 Turner, M. J., McKinnon, J. J., Wolff, S. K., Grimwood, D. J., Spackman, P. R., Jayatilaka, D. & Spackman, M. A. (2017). *CrystalExplorer17*. The University of Western Australia.
 Turner, M. J., Thomas, S. P., Shi, M. W., Jayatilaka, D. & Spackman, M. A. (2015). *Chem. Commun.* **51**, 3735–3738.
 Venkatraman, R. & Fronczek, F. R. (2015). *CSD Communication* (refcode QUDJAC). CCDC, Cambridge, England.
 Vira, J. J., Patel, D. R., Bhimani, N. V. & Ajudia, P. A. (2010). *Pharma Chem.* **2**, 178–183.
 Westrip, S. P. (2010). *J. Appl. Cryst.* **43**, 920–925.

supporting information

Acta Cryst. (2021). E77, 559-563 [https://doi.org/10.1107/S2056989021004291]

Crystal structure, Hirshfeld surface analysis and interaction energy calculation of 1-decyl-2,3-dihydro-1*H*-benzimidazol-2-one

Younesse Ait Elmachkouri, Asmaa Saber, Ezaddine Irrou, Bushra Amer, Joel T. Mague, Tuncer Hökelek, Mohamed Labd Taha, Nada Kheira Sebbar and El Mokhtar Essassi

Computing details

Data collection: *APEX3* (Bruker, 2016); cell refinement: *SAINT* (Bruker, 2016); data reduction: *SAINT* (Bruker, 2016); program(s) used to solve structure: *SHELXT/5* (Sheldrick, 2015*a*); program(s) used to refine structure: *SHELXL2018/3* (Sheldrick, 2015*b*); molecular graphics: *DIAMOND* (Brandenburg & Putz, 2012); software used to prepare material for publication: *pubCIF* (Westrip, 2010).

1-Decyl-2,3-dihydro-1*H*-benzimidazol-2-one

Crystal data

$C_{17}H_{26}N_2O$

$M_r = 274.40$

Monoclinic, $P2_1/c$

$a = 17.3256$ (5) Å

$b = 5.5662$ (2) Å

$c = 16.7244$ (5) Å

$\beta = 97.433$ (1)°

$V = 1599.31$ (9) Å³

$Z = 4$

$F(000) = 600$

$D_x = 1.140$ Mg m⁻³

Cu $K\alpha$ radiation, $\lambda = 1.54178$ Å

Cell parameters from 9927 reflections

$\theta = 2.6\text{--}72.4^\circ$

$\mu = 0.55$ mm⁻¹

$T = 150$ K

Parallelepiped, colourless

$0.26 \times 0.17 \times 0.10$ mm

Data collection

Bruker D8 VENTURE PHOTON 100 CMOS diffractometer

Radiation source: INCOATEC I μ S micro-focus source

Mirror monochromator

Detector resolution: 10.4167 pixels mm⁻¹

ω scans

Absorption correction: numerical (*SADABS*; Krause *et al.*, 2015)

$T_{\min} = 0.88$, $T_{\max} = 0.95$

11457 measured reflections

3082 independent reflections

2857 reflections with $I > 2\sigma(I)$

$R_{\text{int}} = 0.028$

$\theta_{\max} = 72.3^\circ$, $\theta_{\min} = 5.6^\circ$

$h = -19 \rightarrow 21$

$k = -6 \rightarrow 6$

$l = -20 \rightarrow 17$

Refinement

Refinement on F^2

Least-squares matrix: full

$R[F^2 > 2\sigma(F^2)] = 0.041$

$wR(F^2) = 0.101$

$S = 1.08$

3082 reflections

286 parameters

0 restraints

Primary atom site location: dual

Secondary atom site location: difference Fourier map

Hydrogen site location: difference Fourier map

All H-atom parameters refined

$w = 1/[\sigma^2(F_o^2) + (0.0505P)^2 + 0.3296P]$

where $P = (F_o^2 + 2F_c^2)/3$

$(\Delta/\sigma)_{\max} = 0.001$

$$\Delta\rho_{\max} = 0.19 \text{ e } \text{\AA}^{-3}$$

$$\Delta\rho_{\min} = -0.26 \text{ e } \text{\AA}^{-3}$$

Extinction correction: *SHELXL 2018/3*
(Sheldrick, 2015b),
 $F_c^* = kFc[1 + 0.001xFc^2\lambda^3/\sin(2\theta)]^{-1/4}$
Extinction coefficient: 0.0415 (17)

Special details

Geometry. All esds (except the esd in the dihedral angle between two l.s. planes) are estimated using the full covariance matrix. The cell esds are taken into account individually in the estimation of esds in distances, angles and torsion angles; correlations between esds in cell parameters are only used when they are defined by crystal symmetry. An approximate (isotropic) treatment of cell esds is used for estimating esds involving l.s. planes.

Refinement. Refinement of F^2 against ALL reflections. The weighted R-factor wR and goodness of fit S are based on F^2 , conventional R-factors R are based on F, with F set to zero for negative F^2 . The threshold expression of $F^2 > 2\text{sigma}(F^2)$ is used only for calculating R-factors(gt) etc. and is not relevant to the choice of reflections for refinement. R-factors based on F^2 are statistically about twice as large as those based on F, and R- factors based on ALL data will be even larger.

Fractional atomic coordinates and isotropic or equivalent isotropic displacement parameters (\AA^2)

	x	y	z	$U_{\text{iso}}^*/U_{\text{eq}}$
O1	0.04776 (4)	0.28130 (13)	0.44474 (4)	0.0303 (2)
N1	0.05137 (5)	0.31336 (16)	0.58449 (5)	0.0277 (2)
H1	0.0208 (9)	0.449 (3)	0.5834 (8)	0.049 (4)*
N2	0.11079 (5)	0.00636 (15)	0.53573 (5)	0.0257 (2)
C1	0.11866 (6)	-0.02174 (17)	0.61924 (6)	0.0255 (2)
C2	0.15374 (6)	-0.20007 (19)	0.66878 (7)	0.0303 (3)
H2	0.1796 (8)	-0.337 (3)	0.6474 (8)	0.039 (3)*
C3	0.15165 (7)	-0.1745 (2)	0.75149 (7)	0.0337 (3)
H3	0.1783 (8)	-0.300 (2)	0.7883 (8)	0.042 (4)*
C4	0.11570 (7)	0.0218 (2)	0.78254 (7)	0.0332 (3)
H4	0.1157 (8)	0.039 (2)	0.8423 (8)	0.037 (3)*
C5	0.07947 (6)	0.19953 (19)	0.73228 (6)	0.0302 (3)
H5	0.0528 (7)	0.334 (2)	0.7533 (7)	0.033 (3)*
C6	0.08152 (6)	0.17382 (17)	0.65026 (6)	0.0261 (2)
C7	0.06765 (6)	0.20902 (17)	0.51435 (6)	0.0253 (2)
C8	0.13586 (6)	-0.16239 (18)	0.47772 (6)	0.0284 (3)
H8A	0.1186 (7)	-0.327 (2)	0.4909 (7)	0.031 (3)*
H8B	0.1074 (7)	-0.116 (2)	0.4234 (8)	0.030 (3)*
C9	0.22347 (6)	-0.16205 (19)	0.47500 (7)	0.0308 (3)
H9A	0.2512 (8)	-0.205 (2)	0.5293 (8)	0.035 (3)*
H9B	0.2344 (8)	-0.290 (2)	0.4382 (8)	0.035 (3)*
C10	0.25501 (6)	0.0740 (2)	0.44707 (7)	0.0325 (3)
H10A	0.2498 (8)	0.199 (3)	0.4881 (8)	0.042 (4)*
H10B	0.2229 (8)	0.128 (2)	0.3965 (8)	0.038 (3)*
C11	0.33982 (7)	0.0550 (2)	0.43186 (7)	0.0355 (3)
H11A	0.3717 (8)	-0.020 (2)	0.4812 (8)	0.041 (3)*
H11B	0.3434 (8)	-0.060 (3)	0.3859 (8)	0.042 (4)*
C12	0.37542 (7)	0.2942 (2)	0.41212 (8)	0.0371 (3)
H12A	0.3739 (8)	0.409 (3)	0.4593 (8)	0.044 (4)*
H12B	0.3426 (8)	0.369 (3)	0.3659 (8)	0.040 (3)*

C13	0.45872 (7)	0.2725 (2)	0.39272 (8)	0.0374 (3)
H13A	0.4913 (9)	0.197 (3)	0.4389 (9)	0.045 (4)*
H13B	0.4594 (8)	0.161 (3)	0.3467 (9)	0.044 (4)*
C14	0.49438 (7)	0.5123 (2)	0.37418 (8)	0.0383 (3)
H14A	0.4944 (9)	0.622 (3)	0.4218 (9)	0.050 (4)*
H14B	0.4604 (8)	0.589 (3)	0.3278 (8)	0.042 (4)*
C15	0.57697 (7)	0.4932 (2)	0.35263 (8)	0.0383 (3)
H15A	0.6106 (9)	0.409 (3)	0.3983 (9)	0.047 (4)*
H15B	0.5772 (8)	0.385 (3)	0.3040 (8)	0.044 (4)*
C16	0.61285 (7)	0.7340 (2)	0.33601 (8)	0.0416 (3)
H16A	0.6112 (9)	0.842 (3)	0.3852 (9)	0.054 (4)*
H16B	0.5799 (10)	0.814 (3)	0.2910 (9)	0.053 (4)*
C17	0.69572 (9)	0.7119 (3)	0.31580 (10)	0.0540 (4)
H17A	0.7312 (11)	0.646 (3)	0.3640 (11)	0.072 (5)*
H17B	0.6977 (10)	0.598 (3)	0.2673 (10)	0.066 (5)*
H17C	0.7161 (11)	0.872 (4)	0.3005 (11)	0.076 (5)*

Atomic displacement parameters (Å²)

	U^{11}	U^{22}	U^{33}	U^{12}	U^{13}	U^{23}
O1	0.0355 (4)	0.0285 (4)	0.0273 (4)	0.0019 (3)	0.0055 (3)	0.0041 (3)
N1	0.0307 (4)	0.0240 (4)	0.0289 (5)	0.0026 (3)	0.0066 (3)	0.0010 (3)
N2	0.0292 (4)	0.0237 (4)	0.0251 (4)	0.0005 (3)	0.0063 (3)	0.0006 (3)
C1	0.0261 (5)	0.0245 (5)	0.0264 (5)	-0.0041 (4)	0.0051 (4)	-0.0002 (4)
C2	0.0343 (5)	0.0253 (5)	0.0315 (6)	0.0005 (4)	0.0049 (4)	0.0011 (4)
C3	0.0391 (6)	0.0307 (6)	0.0307 (6)	-0.0021 (4)	0.0022 (4)	0.0053 (4)
C4	0.0376 (6)	0.0359 (6)	0.0267 (6)	-0.0055 (4)	0.0061 (4)	0.0006 (4)
C5	0.0329 (5)	0.0288 (5)	0.0301 (6)	-0.0031 (4)	0.0087 (4)	-0.0032 (4)
C6	0.0255 (5)	0.0246 (5)	0.0284 (5)	-0.0035 (4)	0.0049 (4)	0.0012 (4)
C7	0.0255 (5)	0.0231 (5)	0.0279 (5)	-0.0033 (4)	0.0061 (4)	0.0011 (4)
C8	0.0337 (5)	0.0235 (5)	0.0288 (5)	-0.0009 (4)	0.0071 (4)	-0.0030 (4)
C9	0.0340 (6)	0.0294 (6)	0.0299 (6)	0.0050 (4)	0.0072 (4)	0.0000 (4)
C10	0.0321 (5)	0.0309 (6)	0.0355 (6)	0.0020 (4)	0.0080 (5)	0.0003 (4)
C11	0.0336 (6)	0.0365 (6)	0.0376 (6)	0.0025 (5)	0.0090 (5)	0.0021 (5)
C12	0.0339 (6)	0.0375 (6)	0.0408 (7)	-0.0002 (5)	0.0081 (5)	0.0009 (5)
C13	0.0347 (6)	0.0385 (6)	0.0399 (7)	0.0005 (5)	0.0086 (5)	0.0020 (5)
C14	0.0355 (6)	0.0377 (7)	0.0423 (7)	-0.0010 (5)	0.0070 (5)	-0.0013 (5)
C15	0.0366 (6)	0.0370 (6)	0.0423 (7)	-0.0022 (5)	0.0081 (5)	-0.0007 (5)
C16	0.0389 (6)	0.0401 (7)	0.0454 (7)	-0.0055 (5)	0.0037 (5)	-0.0002 (5)
C17	0.0432 (7)	0.0588 (9)	0.0612 (9)	-0.0130 (6)	0.0111 (7)	0.0003 (7)

Geometric parameters (Å, °)

O1—C7	1.2378 (12)	C10—H10A	0.988 (14)
N1—C7	1.3706 (13)	C10—H10B	0.996 (14)
N1—C6	1.3920 (13)	C11—C12	1.5214 (16)
N1—H1	0.923 (16)	C11—H11A	1.021 (14)
N2—C7	1.3747 (13)	C11—H11B	1.009 (14)

N2—C1	1.3944 (13)	C12—C13	1.5245 (16)
N2—C8	1.4564 (12)	C12—H12A	1.017 (14)
C1—C2	1.3823 (14)	C12—H12B	0.989 (14)
C1—C6	1.3981 (14)	C13—C14	1.5197 (16)
C2—C3	1.3958 (16)	C13—H13A	0.990 (15)
C2—H2	0.974 (14)	C13—H13B	0.990 (15)
C3—C4	1.3910 (16)	C14—C15	1.5239 (16)
C3—H3	1.003 (14)	C14—H14A	1.004 (16)
C4—C5	1.3940 (16)	C14—H14B	1.007 (14)
C4—H4	1.004 (13)	C15—C16	1.5182 (17)
C5—C6	1.3841 (15)	C15—H15A	1.014 (15)
C5—H5	0.970 (13)	C15—H15B	1.013 (15)
C8—C9	1.5246 (15)	C16—C17	1.5221 (19)
C8—H8A	0.995 (13)	C16—H16A	1.020 (16)
C8—H8B	1.009 (13)	C16—H16B	0.989 (16)
C9—C10	1.5195 (15)	C17—H17A	1.017 (19)
C9—H9A	1.000 (13)	C17—H17B	1.033 (18)
C9—H9B	0.974 (13)	C17—H17C	1.00 (2)
C10—C11	1.5269 (15)		
O1...N2 ⁱ	3.2324 (11)	H8B...H10B	2.507 (18)
O1...C1 ⁱ	3.2784 (12)	H9A...H11A	2.550 (19)
O1...N1 ⁱⁱ	2.8394 (11)	H9B...H11B	2.53 (2)
C4...O1 ⁱⁱⁱ	3.2820 (14)	H10A...H12A	2.55 (2)
O1...H8B	2.486 (11)	H10B...H12B	2.58 (2)
O1...H1 ⁱⁱ	1.934 (16)	H11A...H13A	2.58 (2)
O1...H8A ^{iv}	2.571 (11)	H11A...H16A ^v	2.43 (2)
H4...O1 ⁱⁱⁱ	2.417 (13)	H11B...H13B	2.51 (2)
N1...C2 ^{iv}	3.4382 (14)	H12A...H14A	2.55 (2)
N1...C8 ⁱ	3.3820 (14)	H12A...H15A ^v	2.57 (2)
N2...C7 ⁱ	3.3206 (14)	H12B...H14B	2.53 (2)
N1...H8A ^{iv}	2.878 (12)	H13A...H15A	2.55 (2)
N1...H8B ⁱ	2.949 (12)	H13A...H14A ^v	2.52 (2)
N2...H10A	2.843 (14)	H13B...H15B	2.57 (2)
C7...C8 ⁱ	3.5550 (15)	H13B...H16B ^{vii}	2.47 (2)
C7...C7 ⁱ	3.2937 (14)	H14A...H16A	2.51 (2)
C2...H17C ^v	2.90 (2)	H14B...H16B	2.56 (2)
C7...H1 ⁱⁱ	2.828 (16)	H14B...H16B ^{vii}	2.54 (2)
C7...H8A ^{iv}	2.774 (11)	H15A...H17A	2.60 (2)
H2...H9A	2.572 (19)	H15B...H17B	2.54 (2)
H2...H17A ^{vi}	2.34 (2)		
C7—N1—C6	110.01 (9)	H10A—C10—H10B	106.7 (11)
C7—N1—H1	120.8 (9)	C12—C11—C10	113.68 (10)
C6—N1—H1	129.0 (9)	C12—C11—H11A	109.9 (8)
C7—N2—C1	109.39 (8)	C10—C11—H11A	109.0 (8)
C7—N2—C8	123.71 (8)	C12—C11—H11B	109.0 (8)
C1—N2—C8	126.57 (8)	C10—C11—H11B	109.0 (8)

C2—C1—N2	131.25 (9)	H11A—C11—H11B	106.0 (11)
C2—C1—C6	121.63 (9)	C11—C12—C13	113.47 (10)
N2—C1—C6	107.11 (8)	C11—C12—H12A	109.2 (8)
C1—C2—C3	117.07 (10)	C13—C12—H12A	109.6 (8)
C1—C2—H2	121.9 (8)	C11—C12—H12B	109.1 (8)
C3—C2—H2	121.0 (8)	C13—C12—H12B	109.3 (8)
C4—C3—C2	121.36 (10)	H12A—C12—H12B	105.9 (11)
C4—C3—H3	120.8 (8)	C14—C13—C12	113.26 (10)
C2—C3—H3	117.9 (8)	C14—C13—H13A	109.1 (8)
C3—C4—C5	121.38 (10)	C12—C13—H13A	109.1 (8)
C3—C4—H4	120.4 (7)	C14—C13—H13B	110.2 (8)
C5—C4—H4	118.3 (7)	C12—C13—H13B	108.7 (8)
C6—C5—C4	117.19 (10)	H13A—C13—H13B	106.1 (12)
C6—C5—H5	120.9 (7)	C13—C14—C15	113.93 (10)
C4—C5—H5	121.9 (7)	C13—C14—H14A	109.3 (9)
C5—C6—N1	132.10 (10)	C15—C14—H14A	109.1 (9)
C5—C6—C1	121.36 (9)	C13—C14—H14B	108.6 (8)
N1—C6—C1	106.55 (9)	C15—C14—H14B	108.7 (8)
O1—C7—N1	127.16 (10)	H14A—C14—H14B	106.9 (12)
O1—C7—N2	125.96 (9)	C16—C15—C14	113.62 (10)
N1—C7—N2	106.88 (8)	C16—C15—H15A	109.7 (9)
N2—C8—C9	113.76 (9)	C14—C15—H15A	108.7 (8)
N2—C8—H8A	108.7 (7)	C16—C15—H15B	109.5 (8)
C9—C8—H8A	109.7 (7)	C14—C15—H15B	109.4 (8)
N2—C8—H8B	106.3 (7)	H15A—C15—H15B	105.7 (12)
C9—C8—H8B	110.2 (7)	C15—C16—C17	112.95 (11)
H8A—C8—H8B	108.0 (10)	C15—C16—H16A	108.4 (9)
C10—C9—C8	114.16 (9)	C17—C16—H16A	110.6 (9)
C10—C9—H9A	109.6 (7)	C15—C16—H16B	109.0 (9)
C8—C9—H9A	109.6 (8)	C17—C16—H16B	109.6 (9)
C10—C9—H9B	109.2 (8)	H16A—C16—H16B	106.0 (13)
C8—C9—H9B	107.1 (8)	C16—C17—H17A	110.1 (11)
H9A—C9—H9B	106.9 (11)	C16—C17—H17B	110.6 (10)
C9—C10—C11	112.56 (9)	H17A—C17—H17B	108.8 (14)
C9—C10—H10A	108.9 (8)	C16—C17—H17C	111.0 (11)
C11—C10—H10A	109.9 (8)	H17A—C17—H17C	109.1 (15)
C9—C10—H10B	109.7 (8)	H17B—C17—H17C	107.1 (14)
C11—C10—H10B	108.8 (8)		
C7—N2—C1—C2	177.13 (10)	C6—N1—C7—O1	177.92 (9)
C8—N2—C1—C2	3.56 (17)	C6—N1—C7—N2	-2.09 (11)
C7—N2—C1—C6	-2.02 (11)	C1—N2—C7—O1	-177.48 (9)
C8—N2—C1—C6	-175.60 (9)	C8—N2—C7—O1	-3.68 (15)
N2—C1—C2—C3	179.89 (10)	C1—N2—C7—N1	2.53 (11)
C6—C1—C2—C3	-1.06 (15)	C8—N2—C7—N1	176.33 (8)
C1—C2—C3—C4	0.11 (16)	C7—N2—C8—C9	111.38 (11)
C2—C3—C4—C5	0.78 (17)	C1—N2—C8—C9	-75.91 (12)
C3—C4—C5—C6	-0.69 (16)	N2—C8—C9—C10	-63.87 (12)

C4—C5—C6—N1	179.37 (10)	C8—C9—C10—C11	-170.56 (9)
C4—C5—C6—C1	-0.26 (15)	C9—C10—C11—C12	-174.11 (10)
C7—N1—C6—C5	-178.81 (10)	C10—C11—C12—C13	-177.01 (10)
C7—N1—C6—C1	0.86 (11)	C11—C12—C13—C14	-179.20 (10)
C2—C1—C6—C5	1.17 (15)	C12—C13—C14—C15	-178.58 (10)
N2—C1—C6—C5	-179.58 (9)	C13—C14—C15—C16	-178.72 (11)
C2—C1—C6—N1	-178.55 (9)	C14—C15—C16—C17	179.15 (11)
N2—C1—C6—N1	0.70 (10)		

Symmetry codes: (i) $-x, -y, -z+1$; (ii) $-x, -y+1, -z+1$; (iii) $x, -y+1/2, z+1/2$; (iv) $x, y+1, z$; (v) $-x+1, -y+1, -z+1$; (vi) $-x+1, -y, -z+1$; (vii) $-x+1, y-1/2, -z+1/2$.

Hydrogen-bond geometry (Å, °)

Cg2 is the centroid of the C1–C6 ring.

<i>D</i> —H \cdots <i>A</i>	<i>D</i> —H	H \cdots <i>A</i>	<i>D</i> \cdots <i>A</i>	<i>D</i> —H \cdots <i>A</i>
N1—H1 \cdots O1 ⁱⁱ	0.923 (16)	1.932 (16)	2.8393 (12)	167.0 (13)
C8—H8 <i>A</i> \cdots O1 ^{viii}	0.995 (13)	2.573 (13)	3.4648 (12)	149.1 (9)
C17—H17 <i>C</i> \cdots <i>Cg2</i> ^v	1.00 (2)	2.985 (19)	3.6656 (17)	126.0 (14)

Symmetry codes: (ii) $-x, -y+1, -z+1$; (v) $-x+1, -y+1, -z+1$; (viii) $x, y-1, z$.